Journal of Marine Science and Technology. Vol. 1, No. 1, pp. 19-22 (1993)

EFFECTS OF ANISOTROPY ON THE HYDROGEN INDUCED FATIGUE CRACK PROPAGATION OF A BANDED FERRITE/PEARLITE STEEL

L. Tau*, S.L.I. Chan* and C.S. Shin†

* *Institute of Materials Science and Engineering*
National Taiwan University
Taipei Taiwan 10764
R.O.C.
†*Department of Mechanical Engineering*
National Taiwan University
mTaipei Taiwan 10764
R.O.C.

Key words: fatigue crack propagation, hydrogen embrittlement, banded structure, inclusion.

ABSTRACT

The fatigue crack propagation (FCP) properties of AISI 4130 steel plates with a ferrite/pearlite (F/P) banded structure were evaluated both in air and electrolytic hydrogen charging environments. To understand the combined effects of hydrogen, directions of banding and elongated non-metallic inclusions on the FCP, specimens with six different orientations relative to the rolling direction were sampled and charged with hydrogen. When tested in air, the result reveals that the crack plane as related to the direction of banding, and the local stress concentration induced by elongated inclusions, largely affected the FCP rate. It also shows that the relative dominance of banding and inclusions depended on the direction of banding. For specimens after hydrogen charging, the results show the FCP rate was an order higher than that for the specimens tested in air. The enhancement of FCP rate was found to vary with respect to the main three directions (longitudinal, transverse and through-surface directions) as related to banding. For specimens where hydrogen can easily diffuse along the longitudinal direction into specimens and assisted crack propagation, they had the highest FCP rate. It was followed by the specimens in which hydrogen diffused along transverse direction. When hydrogen diffused through layers of ferrite

INTRODUCTION

For *Cr-Mo* and *Ni-Cr-Mo* steel plates after hot rolling or controlled rolling, two types of preferred orientation can occur, namely the crystallographic texturing (alignment of crystallographic planes and directions) and mechanical fibering (alignment of grains, chemically segregated areas and inclusions). Thus a typical microstructure of hot rolled *Cr-Mo* and *Ni-Cr-Mo* steel plates usually composed of a structure with alternative layers of banded ferrite and pearlite (F/P) structure [1]. The anisotropy of banded structure due to mechanical fibering is generally manifested by a decrease in tensile ductility, impact resistance and fracture toughness in the long and short transverse directions [2]. In addition, it has been found that at room temperature the main diffusive path for hydrogen in ferrite/pearlite structure is along the ferrite grains or interface between ferrite and pearlite [3]. This means that the hydrogen intake is different in

Table 1. The chemical composition of AISI 4130 steel.

Element	C	Si	Mn	P	S	Ni	Cr	Mo	Fe
wt.%	0.3	0.2	0.41	0.02	0.01	0.04	0.99	0.15	Bal

different directions when banding occurs [4]. Thus the degree of hydrogen embrittlement, as manifested by the loss of ductility, is similar when hydrogen diffuses along the longitudinal and transverse directions. But if the banding is perpendicular to the hydrogen diffusion path, the degree of hydrogen embrittlement is reduced. Above observations make the anisotropic effects of the banding on FCP in air and hydrogen environment interesting [5,6]. On the other hand, elongated sulfide inclusions have been noted to assist short range hydrogen diffusion [7,8] and lead to differences in behavior in hydrogen induced cracking in different orientations [9,10]. It has also been stated that the dissolving of manganese sulfide inclusions in an aqueous hydrogen environment leads to local concentration of H_2S, which can accelerate hydrogen embrittlement [7,11].

In the above investigations the degree of embrittlement was studied under static stress or slow strain rate conditions. The role of banding on the hydrogen induced fatigue cracking has scarcely been mentioned. It was the objective of this work to study the effects of the F/P striations and elongated inclusions in AISI 4130 steel plates on the FCP rate in a hydrogen charging environment.

EXPERIMENTAL PROCEDURES

1. Materials and specimen sampling

The chemical composition of the 32 mm thick AISI 4130 plates used in this study is given in Table 1. The microstructure of as-received material was a typical banded ferrite/pearlite structure (as shown in Fig. 1). The inclusions in banded structure were elongated along the rolling direction (as shown in Fig. 2).

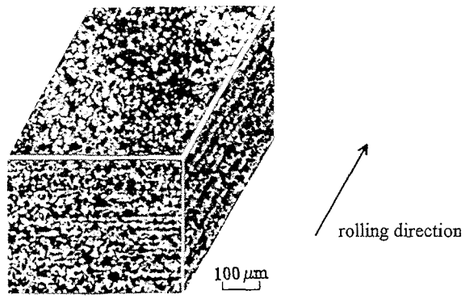

Fig. 1. Micrograph showing the banded ferrite/pearlite structure.

Fatiguecrack propagation tests were performed using the appropriate ASTM specifications[12]. Fatigue specimens of compact-tension type were machined from all six possible orientations: *LS*, *LT*, *TS*, *TL*, *ST* and *SL* orientations as related to the rolling direction (as shown in Fig. 3). The dimensions of these fatigue specimens are: width = 25mm, thickness = 6.25mm.

2. Fatigue Crack Propagation Rate Test

To study the FCP properties of the AISI 4130 steel plates under hydrogen charging, the specimens

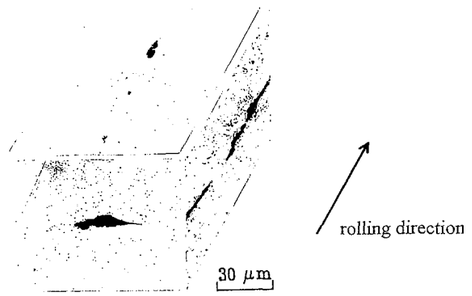

Fig. 2. Micrograph showing the elongated inclusions found in banded structures.

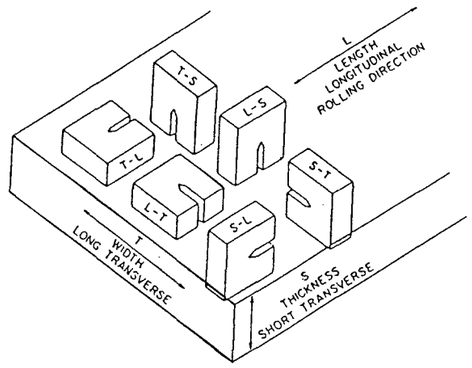

Fig. 3. Schematic diagram showing the sampling orientations of the tested specimens.

were charged in 4Vol.% H_2S0_4 + 20mg As_2O_3/l solutions, with an applied cathodic current density 20A/m². Other conditions of loading were: *R*-ratio = 0.1, P_{max} = 3.5 kNt and loading frequency = 0.5Hz. Fatigue test was also performed in air, with a loading frequency of 20Hz. The FCP data in air have been summarized using the Paris' law, and plots of the FCP data in air were used to contrast with that in the cathodic charged conditions.

RESULTS AND DISCUSSION

1. FCP rate in air

The FCP data of all specimens in air were treated by Paris' law, and the constants are rearranged as in Table 2. As discussed in reference 5, the crack paths of specimens with a banded structure can be divided into three modes. The first mode is for the specimens of *SL* and *ST* orientation, fatigue crack propagated easily along weak interfaces, thus delamination and a higher FCP rate would resulted. The specimens of *TL* and *LT* orientation have a second mode, in which the path of crack was divided by alternate layers of ferrite and pearlite, and this composite-like effect was found to resist FCP rate. The third mode is found in the specimens of *TS* and *LS* orientation, where the crack propagation through direction of thickness would branch easily, and the FCP rate would be lowered. In this work, for the FCP the m value in the Paris' law agreed closely to this viewpoint, except for the specimens of *TL* orientation. The reason for this apparent discrepancy is that the influences on FCP of specimens with a banded structure include both the banding and elongated inclusions. The result reveals that the local stress concentration induced by elongated inclusions, which are parallel to the crack plane, produced a pronounced effect on FCP rate for the specimens of *TL* orientation. Similar observation is found for the *SL* specimens, which have a higher m value as compared with that of *SL* specimens.

Table 2. The parameter C, m in Paris' law : da/dn = C (K) ^{m}, for FCP in air, 20Hz.

orientation		C(mm/cycle, MPa-m$^{1/2}$)	m
banded structure	TL	$7.34*10^{-10}$	3.62
	TS	$1.68*10^{-10}$	3.27
	LT	$1.81*10^{-9}$	3.25
	LS	$2.03*10^{-9}$	3.28
	SL	$4.49*10^{-10}$	3.83
	ST	$6.41*10^{-10}$	3.66

2. FCP rate in hydrogen environment

After hydrogen charging, the FCP rates of all specimens were an order higher than that of the specimens tested in air, regardless of the orientations. The FCP rates in the two environments as represented by a graph of log da/dn versus log Δk, as shown in Fig. 4. It also shows that the variation of FCP rates of different orientations were more significant when hydrogen charged. This was especially so in the zone of higher Δk.

For clarity curves of log da/dn versus log k for specimens charged with hydrogen are shown in Fig. 5.

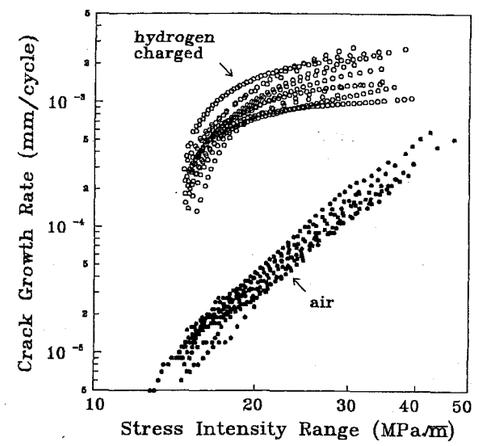

Fig. 4. log da/dn versus log ΔK curve for specimens tested in air and hydrogen environments.

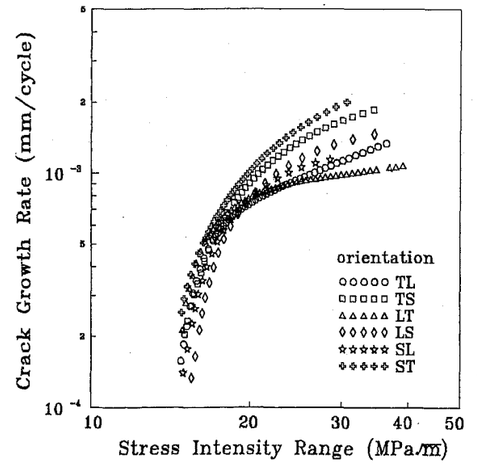

Fig. 5. log da/dn versus log ΔK curve for banded structure in hydrogen environment.

The result shows that the FCP rates of specimens with a banded structure could be divided by three conditions according to their degree of enhancement. Figure 5 shows that specimens of *ST* and *TS* orientations had the highest FCP rate, followed by the specimens of *LS* and *SL* orientations, with the specimens of *TL* and *LT* orientations having the lowest crack propagation rate. As discussed in reference 4, Lee and Chan indicated that the hydrogen permeabilities were different for banded structure. The penetration flux of hydrogen along the longitudinal direction was higher than that along the transverse direction (as shown in Fig. 6),which in turn was faster than that along the through-face direction. Above results suggest that the preferred path for hydrogen diffusion in a banded structure has an important effect on fatigue crack propagation. For the *ST* and *TS* specimens, the faces where hydrogen diffused in have the ferrite/pearlite bands parallel to the hydrogen diffusion path, i.e. along the longitudinal direction. It means that the hydrogen intake was the highest [4] and there was an ample supply of hydrogen to the crack plane. Consequently the FCP rate for the specimens was the highest. On the other hand, for the *T-L* and *L-T* specimens, the hydrogen had to diffuse through bands of ferrite and pearlite, which was obviously more difficult. Thus the FCP rate was the lowest. It has also been found that non-metallic inclusions did not affected very much the FCP rate. As is demonstrated by the *S-L* and *T-L* specimens, both specimens only have a moderate FCP rate compared with the others.

CONCLUSION

1. In air, the alignment of ferrite/pearlite and elongated inclusion both affect the FCP rates of specimens with a banded structure. It was found that the *SL*, *ST*specimens have the highest FCP rates. Inclusions in the *SL* and *TL* specimens were parallel to the crack plane, hence further assisted the FCP rate.
2. In hydrogen environment, the FCP rates of all specimens was an order higher than that when tested in air. The FCP rate was very much depended on the hydrogen diffusion path to the crack tip. When thecrack plane were parallel to the longitu dinal fast diffusion path, the FCP rate was the highest. When the crack plane were perpendicular to the high hydrogen diffusivity path, the FCP rate was found to be lowered.

ACKNOWLEDGMENT

The authors would like to appreciatively acknowledge the support of this work by the National Science Council of Republic of China under Contract no. NSC 79-0405-E-002-18.

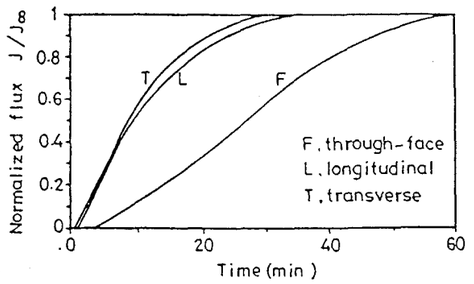

Fig. 6. Normalize output flux of the hydrogen oxidation current of the second polarization transient curve, showing a faster hydrogen penetration along the longitudinal than along the transverse direction, which in turn was faster than that along the through-face direction [4].

REFERENCE

1. Lavender, J.D. and F.W. Jones, J. Iron Steel Inst., London, 9 (1949) 14.
2. Grange R.A., Metall. Trans., 2 (1971) 417.
3. Chan S.L.I. and J.A. Charles, Mater. Sci. Technol., 2 (1986) 956.
4. Lee H.L. and S.L.I. Chan, Mater. Sci. and Eng.,A170 (1991) 193.
5. Heiser F.A. and R.W. Hertzberg, J. of Basic Eng.,June 1971, p.211.
6. Wilson A.D., J. of Engineering Materials and Technology, July 1984, p.233.
7. Pumphrey P. H., Corrosion-NACE, 36 (1980) 537.
8. Pumphrey P.H., Metal Science, 16 (1982) 41.
9. Savage W.F., E.F. Nippes and M.A. Pellman, Welding J., Nov. 1979, p.315.
10. Ven Katasubramanian, T.V. and T.J. Baker, Metal Science, 16 (1982) 543.
11. Vosikovsky O.,J. of Engineering Materials and Technology, Oct. 1975, p.298.
12. 1982 Annual Book of ASTM Standards, E647, ASTM, Philadelphia, 1982.

Journal of Marine Science and Technology. Vol. 1, No. 1, pp. 23-29 (1993)

SECOND LAW ANALYSIS ON EJECTION COOLING SYSTEM

S.P. Liaw and Y.H. Chang
Department of Mechanical and Marine Engineering
National Taiwan Ocean University
Keelung, Taiwan, R.O.C.

Key words: ejector, evaporator, availability, energy.

ABSTACT

Ejection cooling system is analyzed by the second law of thermodynamics in this study. It is mainly consisted of a boiler, an ejector, an expansion device, a condenser, and an evaporator. Special focus is stressed on the variation of exergy in each component. The working refrigerant received exergy from boiler and pump and consumed in other parts of the system. The coefficients of performance based on both the first and the second laws are computed respectively and thus the changes of energy and exergy in each component of the system can be readily understood. In addition, the boiler temperature, evaporator temperature, condenser temperature, nozzle efficiency, and diffuser efficiency are varied parametrically and the results are tabulated. Finally, a compression cooling system operating at the same condition is made to compare with the present results.

INTRODUCTION

From this century on, many scholars [1-3] have engaged in researching and developing new cooling systems to overcome the weakness of conventional air-conditioner. In a conventional refrigeration cycle, it is composed of a compression device, a condenser, an expansion device, and an evaporator. Instead of a mechanical compression device, however, an ejector has recently been used to pump the refrigerant vapor. The thermodynamic mechanism of ejection cooling system is a combination of a Rankine cycle and a refrigeration cycle. The basic feature of it is to produce a suction pressure to drive the refrigeration vapor with the aid of the Rankine cycle. The components are illustrated in Fig.1. The working liquid is heated in the boiler and it enters the ejector at a state with high pressure and high temperature. In the ejector, a vacuum pressure occurs at the throat and it is possible to entrain the low-pressure vapor of refrigerant from evaporator. The mixed flow is decelerated and compressed by converting the kinetic energy into static pressure, thereafter it goes into the condenser in which heat is rejected by a circulating air or water. The liquid refrigerant leaving from the condenser flows partly through an expansion valve to the evaporator where the lower pressure liquid refrigerant is vaporized by absorbing heat from the surroundings to achieve the desired cooling effect, and partly back to the boiler through a pump to form a closed cycle. Since the ejector is driven by the high-pressure refrigerant vapor supplied from a boiler. A low grade thermal resource such as industrial waste heat or solar energy can be utilized in the boiler, thus the thermal analysis on an ejection cooling system becomes fascinating.

The analysis of available energy in each component has invoked considerable interest in these years.

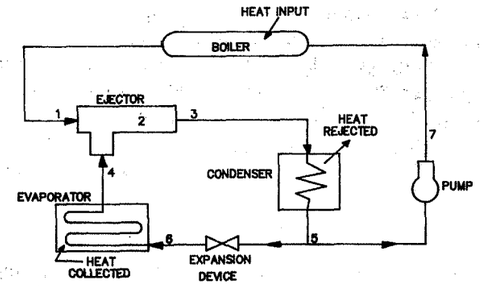

Fig. 1. Schematic diagram of ejection cooling system.